



Numerical and experimental investigation on the performance of the capillary tube using R-134a and R-600a

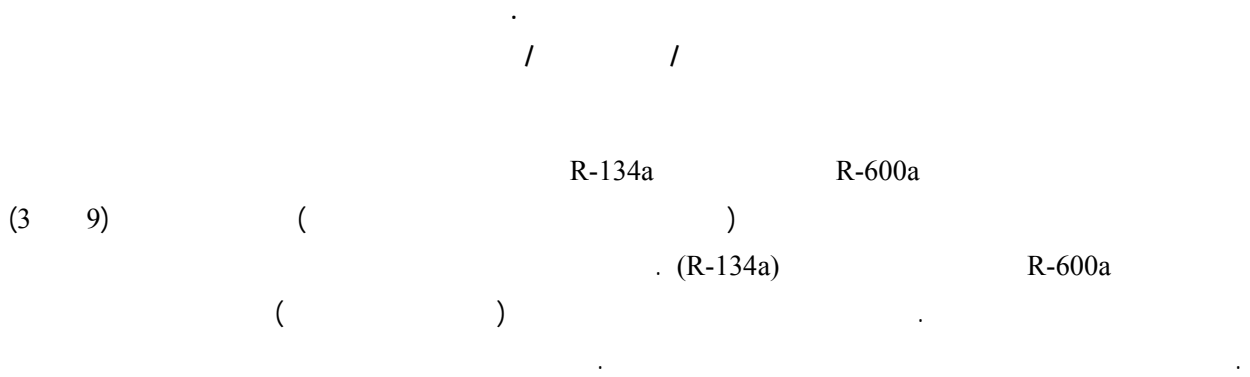
Prof.Dr.Qasim Saleh Mehdi
Mech. Eng. Dept.
College of Engineering
AL-Mustansiriya University
E-mail:qasim60@yahoo.com

Baydaa Jaber Nabhan
Mech. Eng. Dept
College of Engineering
AL-Mustansiriya University
E-mail:Baydaa1971@yahoo.com

Abstract

In this paper, isobutane (R-600a) is used as a suitable substitute for (R-134a) when changing the length of capillary tube. And the experimental data on capillary tube are obtained under different conditions such as (subcooling and ambient temperatures) on domestic refrigerator (9ft3 size), this data shows that (R-600a) a suitable substitute for (R-134a). The test presented a model for a steady state, two-phase flow in capillary tube for vapour compression system. The numerical model depends on conservation equations (mass, energy and momentum) as well as the equation of state for refrigerant. The solution methodology was implemented by using finite difference techniques. The system results indicate that it is possible to change the refrigeration system using (R-134a) by shorter capillary tube length about (28.6%) when using (R-600a). The theoretical results for different variables such as (subcooling and ambient temperatures) showed a good agreement with the "ASHRAE" tables and experimental results.

Key Word: Refrigeration; Capillary Tube; Domestic refrigerator; R-134a; R-600a.



R-600a (28.6%)
"ASHRAE"
R-134a
()
R-600a R-134 :

Introduction

The capillary tube is one type of expansion device used in small vapour compression refrigerating and air conditioning systems. The capillary tube is made from an extremely small-bore hollow copper tube (in the order of 0.5-1.5mm diameter) of about 2-5m length [Bansal and Rupasinghe, 1998]. Liquid refrigerant enters the capillary tube, and as it flow through the tube, the pressure drops because of friction and acceleration of the refrigerant. Its simplicity, low initial cost and low starting torque of compressors are the main reasons for its use.

The flow enters the capillary tube in a subcooled condition, while in a subcooled the pressure drop is linear and the temperature is constant. Once the pressure drops down to saturation condition, a superheated liquid flow is realized for a short distance (metastable region). In this region vapour bubbles appear and pressure suddenly drops. However, this is a metastable region because of the existence of superheat liquid together with saturated liquid and vapour fluid. After this region the local thermodynamic equilibrium state, liquid-vapour two phases is reached as shown in Fig.

(1).Choked flow usually is encountered at the tube exit.

Especially in the past 20 years or so, the flow characteristics of refrigerant passing through capillary tubes have been widely studied experimentally or analytically with alternative and common traditional refrigerants.

Koizumi and Yokoyama (1980), measured pressure and temperature distributions for refrigerant R-22 flow in adiabatic capillary tubes, verifying the occurrence of the delay of vaporization. The authors proposed a simple calculation method to find the length of the liquid region. Such method was developed for adiabatic flow, based on integration of the momentum equation and assuming two-phase homogeneous flow. The experimental results showed a delay of vaporization ranging from 2°C to 4°C and the average length of the metastable flow was 0.39m. The maximum length was 0.6m, and calculations agree with experimental data within ±3%.

Li et al. (1990), investigated the effects of the diameter, back pressure, subcooling degree and mass flow rate on metastability for R-12. It was found that a decrease in the length of



metastable flow region as the capillary tube diameter increases. The mass flow rate increased as consequence of a larger underpressure of vaporization ΔP_{vap} , and an increase in ΔT_{sub} caused a decrease in ΔP_{vap} . It was also verified that the position of the flashing inception was not affected by backpressure variations.

Chen et al. (1990), developed a correlation for the delay of vaporization for R-12 flow through capillary tube based on the nucleation theory initially developed by Alamgir and Lienhard (1981) and with experimental data of Li et al. (1990). For instance, Dirik et al. (1994) verified that Chen's correlation was suitable for R-134a flow through capillary tubes, and Bittle and Pate (1996) used such correlation for R-22, R-134a, R-152a and R-410A.

Valladares et al. (2002), showed that the importance of considering the metastable region in the mathematical model gives more accurate mass flow rate predictions. Results presented included both metastable flow modeling and non-metastable flow modeling. Also homogeneous and separated flow model for metastable flow was presented using different empirical correlation which was essential in the numerical model.

Li Yang and Wen Wang (2007), studied a generalized correlation for predicting the refrigerant mass flow rate through the adiabatic capillary tube with approximate

analytic solutions based on the extensive data for R-12, R-22, R-134a, R-290, R-600a, R-410A, R-407C, and R404A, in which a homogeneous equilibrium model for two-phase flow was employed. The predicted values from the correlation agree well with the experimental data for those seven refrigerants.

The aim of this paper is to evaluate the overall performance of the refrigeration system, in the steady state condition through experimental and theoretical modeling using R-134a and R-600a. The work will also include the following points:

1. Investigating the performance of alternative refrigerant R-600a to be used in the same system.
2. Analyzing the experimental data for various conditions for flow in an adiabatic capillary tube using Bourdon gauge to measure pressure, and using thermocouple type (T) to monitor temperature, along the capillary tube.
3. Comparing the calculation results with experimental results.

Mathematical Model

The pressure distribution pattern along a tube depends on a many factors such as the tube geometry (i.e. tube length, inner diameter, roughness) and refrigerant entrance conditions (i.e. condensing pressure, degree of sub-cooling and/or quality). The mass flow rate has

Significant influence on the fluid flow, especially in the two-phase region and affects the pressure drop and quality of the refrigerant. The exit condition, either choked or unchoked, also depends considerably on the mass flow rate. For a given condensing pressure and tube length, the mass flow rate through the capillary tube remains constant for evaporating pressure lower than the choke value. **Fig. (2)** shows the schematics of typical capillary tube.

The following assumptions are made in this model:

- Straight horizontal and constant inner diameter and roughness capillary tube,
- One-dimensional flow,
- Adiabatic and homogeneous two-phase flow,
- The flow in the single-phase metastable region is considered,
- Thermodynamic equilibrium through the capillary tube.

According to the assumption above, the governing equations used in describing the flow are presented as follows:

I. Entrance Region

In this region losses due to sudden contraction and dynamic pressure head losses, magnitude of this drop is calculated from equation: [Fatouh, 2007]

$$\Delta P_c = (G)^2 \left(\frac{1}{2\rho_{SL}} \right) \left(\frac{1}{C_{con}} - 1 \right)^2 \quad (1)$$

The contraction coefficient (C_{con}) is correlated as a function of area ratios (A_2/A_1) in the following form:

$$C_{con} = 0.6083 + 0.547 \left(\frac{A_2}{A_1} \right) - 0.326 \left(\frac{A_2}{A_1} \right)^2 + 0.168 \left(\frac{A_2}{A_1} \right)^3 \quad (2)$$

Where A_1 and A_2 are the cross section area of the condenser outlet tube and the capillary tube, respectively.

II. Single -Phase (Sub-Cooled Liquid) Region

In this region, the fluid is assumed to be incompressible and steady. Also pressure drop is linear, and the refrigerant is entirely in the liquid state. The capillary tube length in the single-phase (subcooled) region can be given by: [Bansal and Wang, 2004]

$$L_{s,p,sub} = \left[\frac{\rho}{G^2} (P_{cond} - P_{sat}) - d_c (k_i + 1) \right] / f_{sp} \quad (3)$$

Where (k_i) is the entrance loss coefficient (for square edged, $k_i=0.5$) and (f_{sp}) is the single-phase friction factor.

(k_i) can be determined from: [Bansal and Wang, 2004]



$$k_i = 0.42 \left[\left(1 - \frac{d_c}{D_{cond.}} \right)^2 \right] \quad (4)$$

for $(d_c/D_{cond.}) < 0.76$

(f_{sp}) can be determined from:

[Churchill, 1977]

$$f_{sp} = 8 \left[\left(\frac{8}{Re_{sp}} \right)^{12} + \frac{1}{(A_{sp} + B_{sp})^{3/2}} \right]^{1/12} \quad (5)$$

Where:

$$A_{sp} = \left[2.457 \ln \left(\frac{1}{\left(\frac{7}{Re_{sp}} \right)^{0.9} + 0.27 \frac{e}{d_c}} \right) \right]^{16} \quad (6)$$

$$B_{sp} = \left(\frac{37530}{Re_{sp}} \right)^{16} \quad (7)$$

$$Re = \frac{\rho U d_c}{\mu_f} = \frac{G d_c}{\mu_f} \quad (8)$$

$$G = \frac{\dot{m}}{A} = \rho U = \text{constant} \quad (9)$$

III. Single-Phase Metastable Region

The delay of vaporization has been observed from some experiments [Mikol,

1963], [Koizumi and Yokoyama, 1980] and [Li et al., 1990], which means that vaporization does not occur at P_s but at some point (P_v) below it, which is also known as the non-thermodynamic equilibrium. The capillary length in this region is known as the metastable length. [Chen et al., 1990] studied the flow through capillary tubes and presented a correlation to predict the underpressure ($P_s - P_v$). It is as follows:

$$\frac{(P_s - P_v) \sqrt{k_a T_{sat}}}{\sigma^{1.5}} = 0.679 \left(\frac{v_{g1}}{v_{g1} - v_{f1}} \right) Re^{0.914} \left(\frac{\Delta T_{sub}}{T_c} \right)^{-0.208} \left(\frac{d_c}{D} \right)^{-3.18} \quad (10)$$

Where D is the reference length.

$$= \sqrt{\frac{k_a T_{sat}}{\sigma}} \times 10^4 \quad (11)$$

The metastable length can then be given by:

$$L_{meta} = (P_s - P_v) \cdot 2 d_c \rho_{sp} / f_{sp} G^2 \quad (12)$$

The metastable length generally decreases with the degree of sub-cooling and increases with increasing condenser temperature, increasing tube inner diameter.

[Bansal and Wang, 2004]

IV. Region Equilibrium Two-Phase Region

[Stoecker & Jones, 1982] and [Bansal and Rupasinghi, 1998] presented a flow model through the two-phase region based on conservation of mass, energy and momentum.

Their models will be regarded in this study. Consider a control volume in the two-phase region as shown in **Fig. (2)**. The conservation of mass can be expressed as follows:

$$\dot{m} = \rho AU = \text{constant} \quad (13)$$

$$\frac{\dot{m}}{A} = \rho U \quad (14)$$

$$U = \frac{G}{\rho} = Gv \quad (15)$$

For steady-state adiabatic with no external work and neglecting the elevation difference, the conservation of energy can be expressed as follows:

$$h + \frac{U^2}{2} = \text{constant} \quad (16)$$

The fluid enthalpy and specific volume are determined by the following equations:

$$h = (1 - \chi)h_f + \chi h_g \quad (17)$$

$$v = (1 - \chi)v_f + \chi v_g \quad (18)$$

Considering the energy balance between point (1) and any point along the capillary tube in two-phase flow region, substituting

equations (17) and (18) into equation (16) gives:

$$h_1 + \frac{U_1^2}{2} = h_f + \chi(h_g - h_f) + \frac{G^2}{2}(v_f(1 - \chi) + v_g\chi)^2 \quad (19)$$

Expanding the right-hand side and rearranging gives:

$$[(v_g - v_f)^2 \frac{G^2}{2}] \chi^2 + [G^2 v_f (v_g - v_f) + (h_g - h_f)] \chi + [\frac{G^2 v_f^2}{2} - h_1 - \frac{U_1^2}{2} + h_f] = 0 \quad (20)$$

This is in the form of a quadratic equation in which the quality (χ) can be expressed as:

$$\chi = \frac{-h_g - G^2 v_f v_{fg} + \sqrt{(G^2 v_f v_{fg} + h_g)^2 - (2G^2 v_f^2) [\frac{G^2 v_f^2}{2} - h_1 - \frac{U_1^2}{2} + h_f]}}{G^2 v_{fg}^2} \quad (21)$$

Where $h_{fg} = h_g - h_f$, and $v_{fg} = v_g - v_f$

The conservation of momentum can be expressed by again considering the element of fluid as shown in **Fig. (3)**.

The sum of the pressure forces acting on the left and the right ends and the shear force acting on the inner pipe wall is equal to the time rate of change of linear momentum of the system. Therefore,

$$(P \frac{\pi d_c^2}{4}) - (P + dP) \frac{\pi d_c^2}{4} - \tau_w \pi d_c dL = \dot{m} dU \quad (22)$$

Where τ_w is the wall shear stress and defined as:

$$\tau_w = f_{tp} \frac{\rho U^2}{8} \quad (23)$$

On rearranging, we get:

$$dL = -\frac{d_c}{f_{tp}} \left[\frac{2dp}{\rho U^2} + \frac{2\dot{m}dU}{A\rho U^2} \right] \quad (24)$$

For a constant mass flow rate such that $d\dot{m} = 0$, we have:

$$-\frac{dU}{U} = \frac{d\rho}{\rho} \quad (25)$$



Substituting equation (25) into equation (24) gives:

$$dL = \frac{2d_c}{f_{tp}} \left[\frac{-\rho dp}{G^2} + \frac{d\rho}{\rho} \right] \quad (26)$$

The capillary tube between points (1) and (4) can be divided into numerous sections as shown in **Fig. (4)**.

The two-phase friction factor (f_{tp}) can be calculated from [**Lin et al., 1990**] correlation as given:

$$f_{tp} = \phi_i^2 f_{sp} \left[\frac{v_{sp}}{v_{tp}} \right] \quad (27)$$

Where f_{sp} is calculated from equation (5).

ϕ : Friction multiplayer is given by:

$$\phi^2 = \left[\frac{8}{\text{Re}_{tp}} + \frac{1}{(A_{tp} + B_{tp})^{3/2}} \right]^{1/2} \left[1 + \chi \left(\frac{v_g}{v_f} - 1 \right) \right] \quad (28)$$

Where: The two-phase Reynolds number is defined by:

$$\text{Re}_{tp} = \frac{U d_c}{\mu_{tp} v_{tp}} \quad (29)$$

Where:

$$U = G \cdot v_{tp} = G(\chi v_g + (1 - \chi)v_f) \quad (30)$$

Dynamic viscosity (μ_{tp}) can be determined from: [**Beattie and Whalley, 1981**]

$$\mu_{tp} = \alpha_{tp} \mu_g + \mu_f (1 - \alpha_{tp})(1 + 2.5\alpha_{tp}) \quad (31)$$

Where: $\alpha_{tp} = \frac{\chi v_g}{v_f + \chi v_{fg}} \quad (32)$

Thus from equation (26), the two-phase length can be expressed as: [**Wongwises and Pirompak, 2001**].

$$L_{tp} = d_c \left[\frac{-2}{G^2} \int_{P_1}^{P_4} \frac{\rho}{f_{tp}} dp + 2 \int_{P_1}^{P_4} \frac{d\rho}{\rho f_{tp}} \right] \quad (33)$$

Thus, total capillary tube length is the summation of the above three lengths in the three different regions as:

$$L_{Tot} = L_{sp,sub} + L_{meta} + L_{tp} \quad (34)$$

The pressure drop in two-phase region can be calculated from the equation: [**Ahmed, 2001**]

$$P_i - P_{i+1} = \frac{f_{tp} G^2 L_{tp}}{2d_c} \left[v_f + \frac{\chi_i + \chi_{i+1}}{2} v_{fg} \right] + G^2 v_{fg} (\chi_{i+1} - \chi_i) \quad (35)$$

Experimental Apparatus and Measurements

The experimental test rig includes the actual refrigeration system (domestic refrigerator in size 9ft³) which was originally manufactured to work with R-134a. A schematic diagram of a single door domestic refrigerator with the instruments and their locations has been shown in **Fig. (5)**.

The apparatus was designed to allow simultaneous control of the pressure and temperature of the liquid entering the capillary tube and also the evaporator pressure. The pressure distribution along capillary tube was measured by precision Borden type gauges. And temperature measurement of the flowing

refrigerant was made by (copper/constantan) thermocouples type's (T). Refrigerant temperatures were measured by mounting thermocouple's probe directly into a groove through the capillary tube wall. The selected capillary tube specifications are (0.82mm) and (2.28mm) inside and outside diameters respectively, with long (2.8m) for R-134a. This length of capillary tube was calculated theoretically, based on a constant inner diameter of the capillary tube. With respect to R-600a, the capillary tube length has been changed several times until the desired evaporator pressure was reached.

As a result to the delay of vaporization phenomenon, and to find the underpressure of vaporization, pressure and temperature sensors must be installed along the capillary tube. In order to measure the pressure drop along the capillary tube, pressure taps were made in the wall of capillary tube using (T) joint. **Fig. (6)** shows a photo of the (T) joint.

The capillary tube cuts into parts, each two parts connected by (T) joint. A (T) joint (Brass covered with chromium) consist of two parts, the first one is a tube with (3.4mm) , (4mm) inside and outside diameters , respectively. This part is connected two parts of capillary tube by solder. The second one is also a tube with (3.4mm), (4mm) inside and outside diameters respectively. This part is constructed with a broad ends contains flair,

which was connected to pressure gauge in order to have a closed chamber.

Results and Discussion

1. Computation Results

The mathematical sample for simulation of capillary tube in adiabatic flow depends on dividing the tube into three regions [liquid (single-phase), delay of vaporization (metastable) and two-phase flow] regions.

Figs (7), (8), (9) and (10) show the distribution of pressure and temperature along capillary tube for R-134a and R-600a, respectively. Pressure and temperature distribution for these figures were plotted at variable degree of subcooling. It can be noticed that as subcooling degree increases, then liquid region length increases, while in metastable and two-phase regions are decreases. Also, the liquid region length for R-134a is less than that for R-600a, while metastable region length and two-phase region length for R-134a are higher than that for R-600a.

Figs (11), (12), (13) and (14) show the effect of different ambient temperatures on (p-h) diagram at constant subcooling temperature difference of (3°C) and (8°C) for R-134a and R-600a, respectively.

2. Experimental Results

Fig. (15) shows increase of COP with superheat (suction temperature) where



subcooling degree is constant. It was observed that COP value for R-134a is lower than that for R-600a.

Fig.(16) shows the underpressure of vaporization (p_s-p_v) as a function of the mass flow rate. It was observed that at a fixed subcooling condition, the underpressure of vaporization increases with an increase of the mass flow rate. This is because of the specific volume for refrigerant vapour. Also, it can be shown that underpressure of vaporization for R-600a is less than that for R-134a in the same system, where R-600a has specific volume for vapour higher than that for R-134a.

Fig. (17) shows that the underpressure of vaporization is a function of the subcooling degree for refrigerant. It can be seen that the underpressure of vaporization decreases with an increase in the subcooling of the refrigerant, ΔT_{sub} . ranges (3-13°C). This is because of the pressure drop in a single-phase region.

Figs (18) and (19) show the pull down time for R-134a and R-600a in the refrigerator freezer and refrigerator cabin, respectively. Pull down time is defined as the time required for changing the freezer air temperature from ambient condition 303K (30°C) to the desired final temperature 261K (-12°C) and the temperature of the air in the cabin should be maintained at 279K (6°C) according to ISO standard for the considered refrigerator class [**Mohanraj et al, 2002**].

The time required to reach the required freezer air temperature of nearly (-12°C) for R-134a and R-600a are approximately (110 and 90 min) respectively. Moreover, the time required to reach the required cabin air temperature of nearly (6°C) for R-134a and R-600a are approximately (95 and 83 min) respectively. And as a result, it can be noticed that the pull down time (to reach steady state) for R-600a less than that of R-134a.

Figs. (20) and (21) show the difference in COP for refrigerants with ambient temperature and subcooling degree. It can be observed that COP of the system decreases with increasing ambient temperature. However, the COP of the system increases with increasing subcooling degree (and constant superheating degree ΔT_{sup}). And as a result, it can be concluded that COP of the system using by R-600a is higher than that of R-134a. This is because of the R-600a operating with condensing pressures less than that of R-134a at different ambient temperatures leading to less power consumption for R-600a when compared with R-134a.

Conclusions

- (1) Through the theoretical results, it was noticed the following:
 - a. R-600a has operating pressures lower than that for R-134a at different working temperatures.

- b. Pressure ratio for R-134a close to pressure ratio of R-600a.
- c. The refrigeration system using R-600a has COP (5%) higher in comparison with R-134a.
- d. The refrigeration system using R-600a has volumetric capacity lower than that for R-134a.
- e. The refrigeration system using R-600a has a discharge temperature lower than that for R-134a and the increase in refrigerant subcooling allows for lowering the discharge temperature which may increase the compressor life

(2) Through the experimental results, it was noticed the following:

- a. COP for the system working by R-600a is higher than that for R-134a at different ambient temperatures and subcooling degrees.
- b. Power consumption for the system working by R-134a is higher than that for R-600a.
- c. Capillary tube used for R-600a must be shorter than that used for R-134a about (28.6%) for the same system.
- d. The underpressure of vaporization decreases with an increase subcooling degree.

Numerical and experimental investigation on The performance of the capillary tube using R-134a and R-600a

- e. The underpressure of vaporization for R-600a during its passage through capillary tube is less in comparison with R-134a.
- f. Pull down time for R-600a is less than that for R-134a.

References

- Ahmed Abdul-Nabi Omran, 2001, "**Comparative Performance of Refrigerants R-22 & R-290 in Vapour Compression System and Steady the effects on the Capillary tube**". M.Sc. Thesis, University of Technology.
- Bansal, P.K., Rupasinghi, A.S., 1998, "**A homogeneous model for adiabatic capillary tubes**". Applied thermal engineering, vol. 18, pp. (207-219).
- Bansal, P.K., Wang, G., 2004, "**Numerical analysis of choked refrigerant flow in adiabatic capillary tubes**". Applied thermal engineering, vol. 24, pp. (851-863).
- Beattie, D.R.H. and Whalley, P.B., 1981, "**A simple two phase Frictional Pressure Drop Calculation Method**". International Journal of Multiphase Flow, vol. 8, pp. 83-87.
- Chen, Z.H., Li, R.Y., Chen, Z.Y., 1990, "**A correlation for metastable flow of refrigerant R-12 through capillary tubes**". ASHRAE Trans., vol. 96, pp. (550-554).



- Churchill, S.W., 1977, "**Frictional equation spans all fluid flow regions**". Chemical Engineering, vol. 84, pp. (91-92).
- Fatouh, M., 2007, "**Theoretical investigation of adiabatic capillary tubes working with propane/ n-butane/ isobutene blends**". Energy Conversion and Management, vol. 48, pp. (1338-1348).
- Koizumi, H., Yokoyama, K., 1980, "**Characteristics of refrigerant flow in a capillary tube**". ASHRAE Trans., vol. 86, pt. 2, pp. (19-27).
- Li, R.Y., Chen,Z.H.,Lin,S.,Chen,Z,Y., 1990, "**Metastable flow of R-12 through capillary tubes**". International Journal of Refrigeration, vol. 13, pt. 3, pp. (181-186).
- Li Yang and Wen Wang, 2007, "**A generalized correlation for the characteristics of adiabatic capillary tubes**". International Journal of Refrigeration, pp. (1-7).
- Lin, S., Li,R.Y.andChen,Z.H., 1990, "**Nnumerical modelling of thermodynamic non-equilibrium flow of refrigerant through capillary tubes**". ASHRAE Transaction, vol.96, pt. 1, pp. (542-549).
- Mikol, E.P., 1963, "**Adiabatic Single and Two-Phase Flow in Small Bore Tubes**". ASHRAE Trans., vol. 5, pp. (75-86).
- Mohanraj, M.,Jayaraj,S.and Muraleedharan,C., 2002, "**Improved Energy Efficiency for HFC-134a Domestic Refrigerator Retrofitted with Hydrocarbon Mixture HC-290/HC-600a) as Drop in Substitute**". National Institute of Technology, Calicut.
- Stoecker, W.F., and Jones, J.W., 1982, "**Refrigeration and Air Conditioning**". Mc Graw Hill, New York.
- Valladares, O.G., Segarra,C.D.and OlivaA., 2002, "**Numerical simulation of capillary tube expansion devices behavior with pure and mixed refrigerants considering metastable region**". Applied Thermal Engineering, vol. 22, pp. (379-391).
- Wongwises, S., and Pirompak, W., 2001, "**Flow Characteristics of pure Refrigerants and Refrigerant Mixtures in Adiabatic Capillary Tubes**". Applied Thermal Engineering, vol. 21, pp. (845-861).

Nomenclature

A : Area (m²)

α : Void fraction

C_{con} : Contraction coefficient (-)

D[\] : Reference length (m)

D_{cond}: Condenser inner diameter (m)

e : Inner surface roughness (mm)

f : Friction factor (-)

G : Mass flux (kg/m².s)

h : Specific enthalpy (kJ/kg)

jd_c : Capillary tube inner diameter (m)

k_a : Boltzmann's constant (J/k)

k_i : Entrance loss coefficient (-)
 L : Length (m)
 \dot{m} : Mass flow rate (kg/s)
 P : Pressure (N/m² (pa))
 ΔP_c : Pressure drop due to the area contraction
(N/m²)
 Re : Reynolds number (-)
 T : Temperature (°C)
 U : Velocity (m/s)
 v : Specific volume (m³/kg)
 χ : Dryness fraction (-)

ϕ : Friction multiplayer (-)

Subscripts

c : Critical value
 $cond$: Condenser
 f : Liquid phase
 g : Vapour phase
 i : Present reading according to element
number
 $i+1$: Next reading
 $meta$: Metastable
 sat,s : Saturated
 sp : Single-phase
 sub : Subcooling
 tp : Two-phase
 Tot : Total
 v : Vapour

Greek Symbols

ρ : Density (kg/m³)
 μ : Dynamic viscosity (kg/m.s)
 σ : Surface tension (N/m)
 τ_w : Shear stress at wall (N/m²)

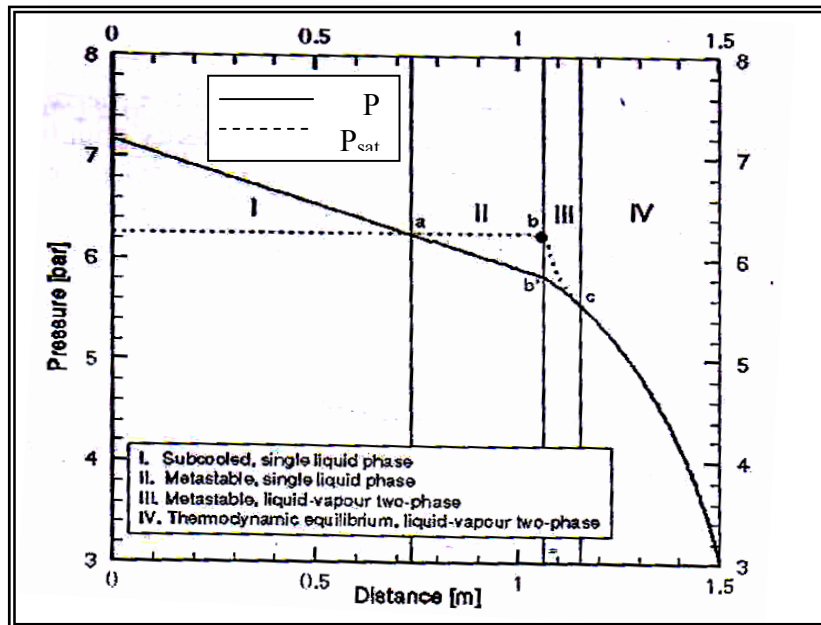


Figure (1): Typical pressure distribution along an adiabatic capillary tube.

[Valladares, 2004]

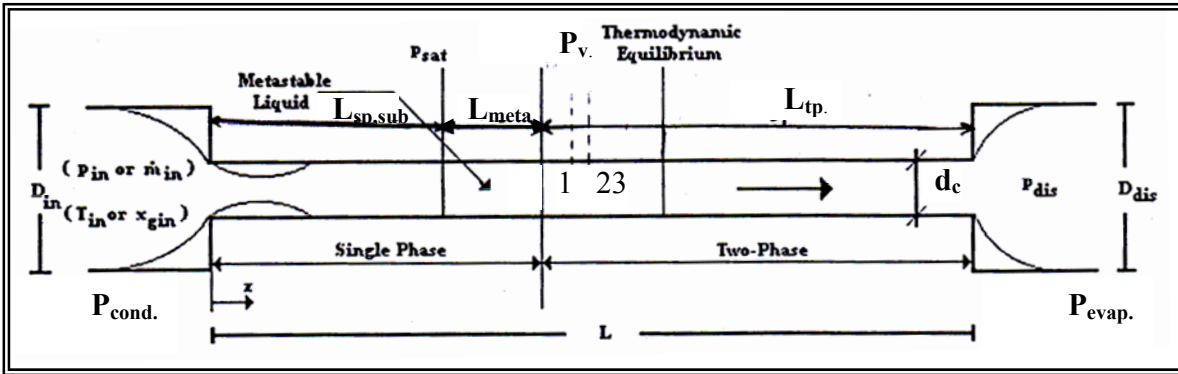


Figure (2): Schematic diagram of a capillary tube [Valladares, 2004]

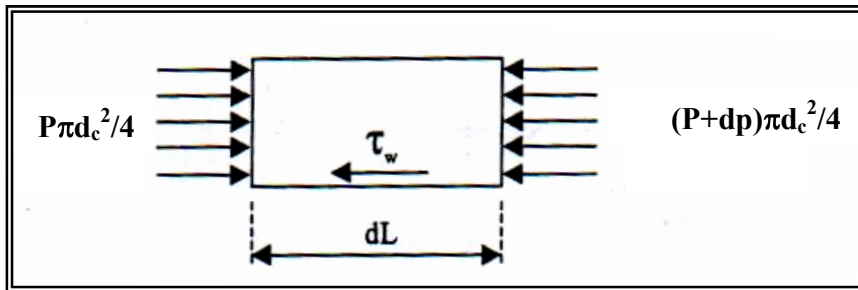


Figure (3): Flow model incremental volume, (two-phase). [Wongwises, Pirompak, 2001]

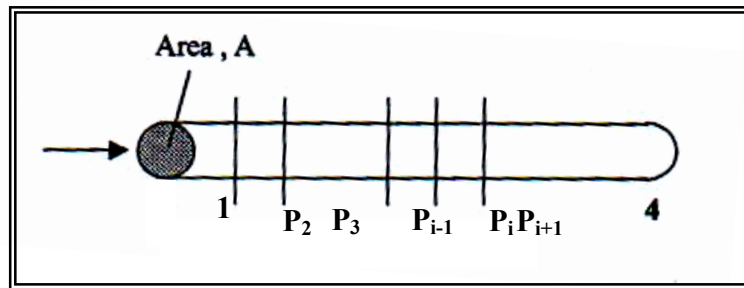


Figure (4): Schematic diagram of simulation approach, (two-phase). [Wongwises, Pirompak, 2001]

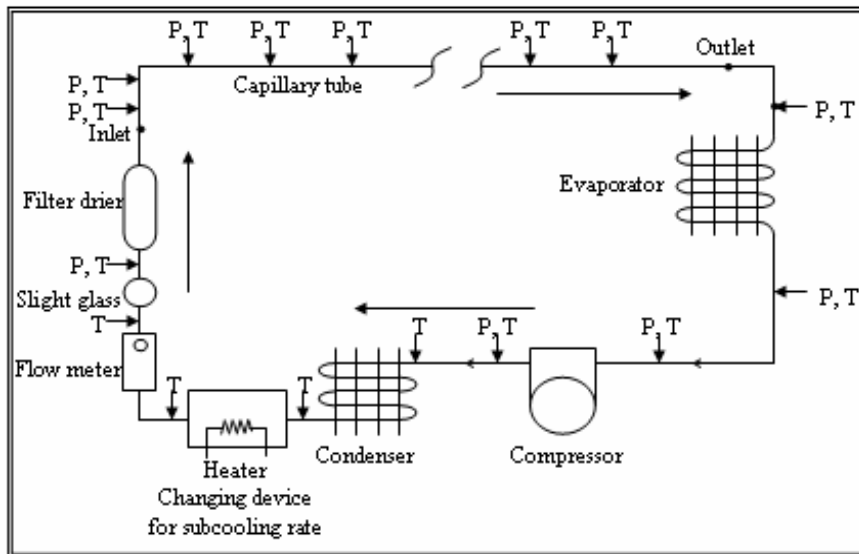


Figure (5): Schematic diagram of the experimental set-up. (Domestic refrigerator). Where: P: Pressure gauge & T: Thermocouple.

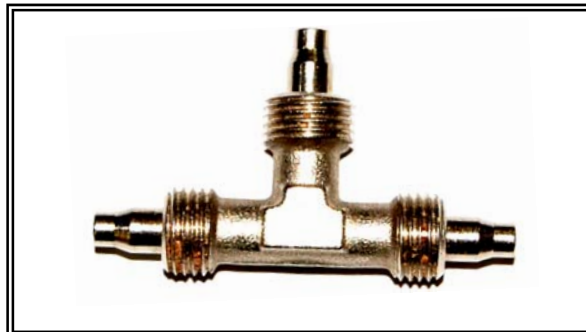


Figure (6): Photo of (T) joint.

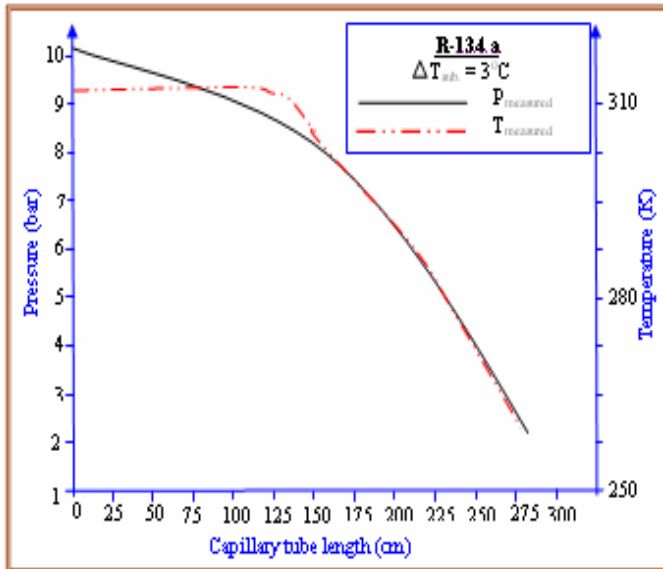


Figure (7): Distribution the pressure and temperature for R- 134a along the capillary tube with $\Delta T_{sub} = 3^{\circ}C$.

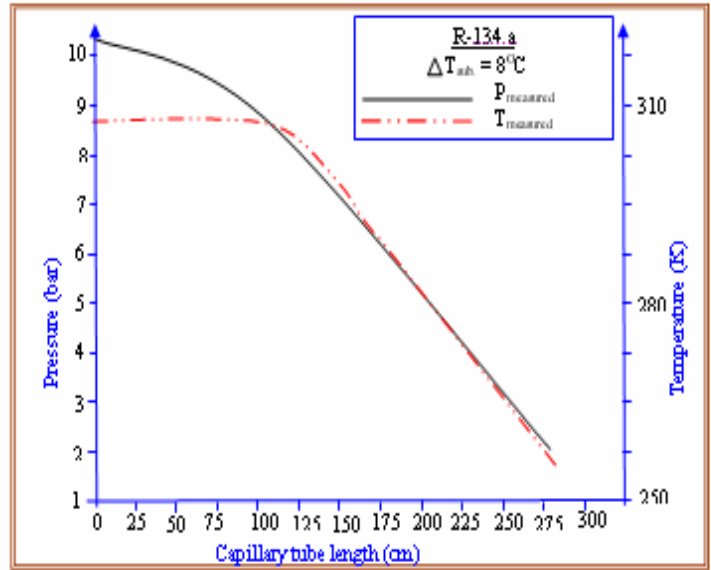


Figure (8): Distribution the pressure and temperature for R-134a along the capillary tube with $\Delta T_{sub} = 8^{\circ}C$.

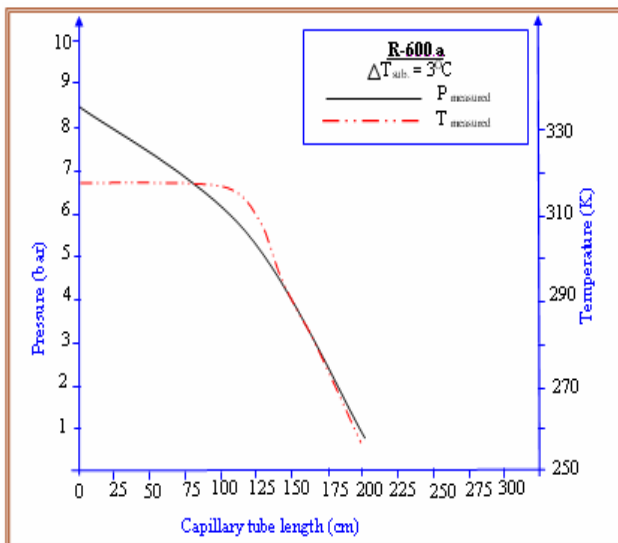
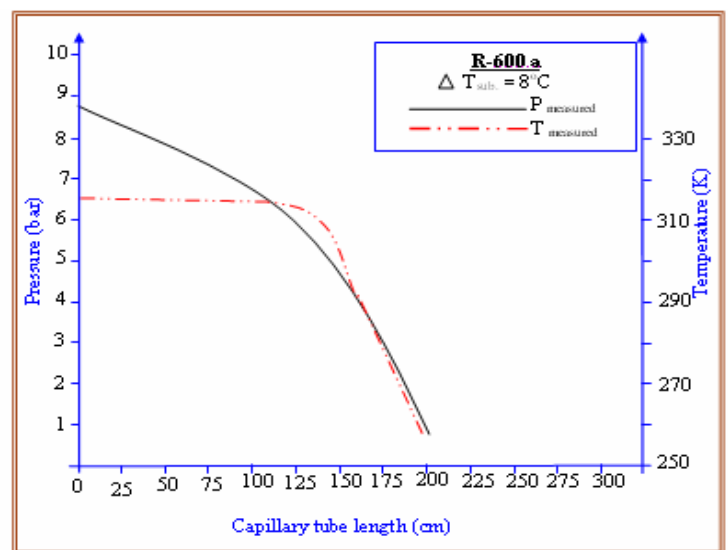


Figure (9): Distribution the pressure and temperature for R-600a along the capillary tube with $T_{sub} = 3^{\circ}C$.



Figure(10): Distribution the pressure and temperature for R-600a along the capillary tube with $T_{sub} = 8^{\circ}C$

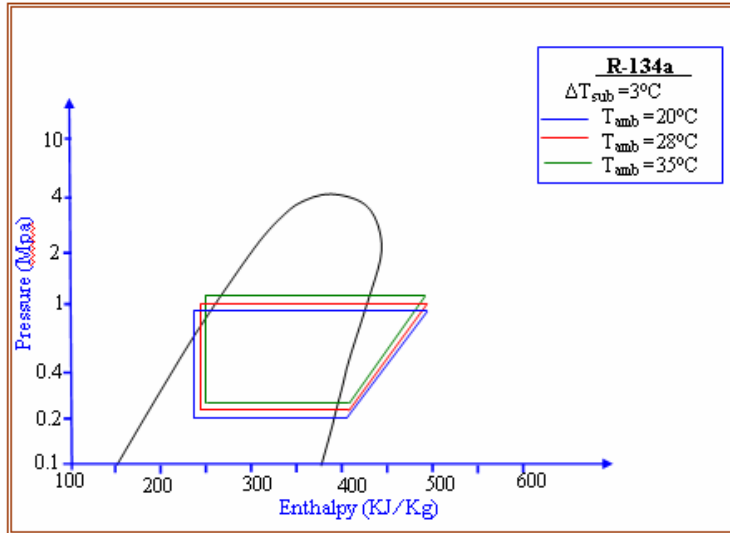


Figure (6.11): Effect of different ambient temperatures on (p-h) diagram at $\Delta T_{sub} = 3^\circ\text{C}$ for R-134a.

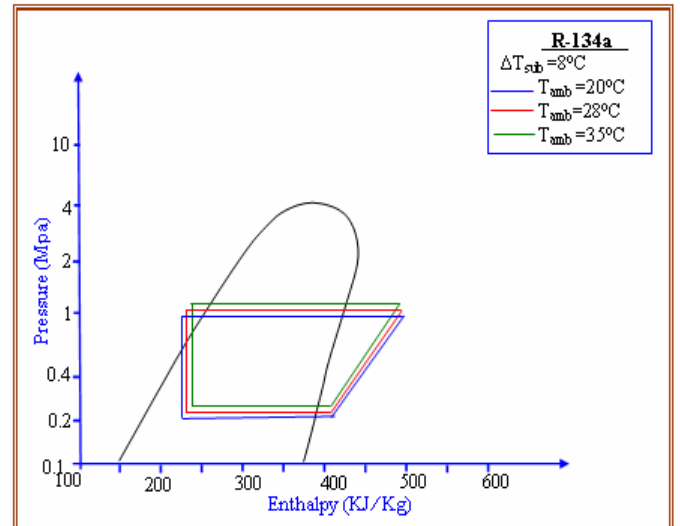


Figure (6.12): Effect of different ambient temperatures on (p-h) diagram at $\Delta T_{sub} = 8^\circ\text{C}$ for R-134a.

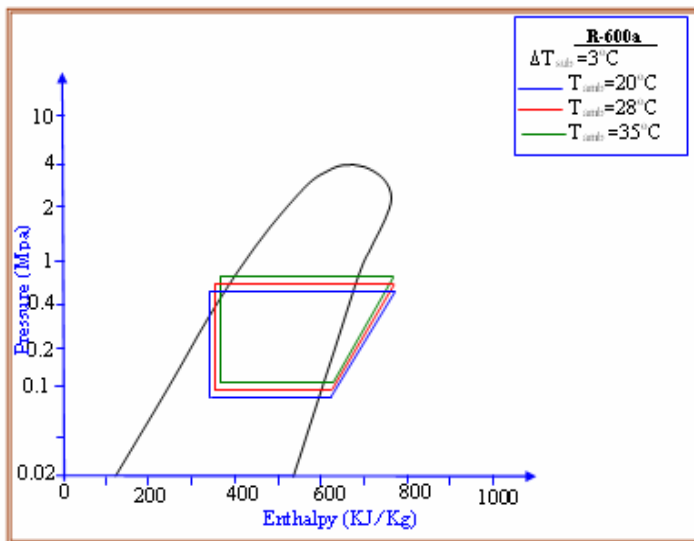


Figure (6.13): Effect of different ambient temperatures on (p-h) diagram at $\Delta T_{sub} = 3^\circ\text{C}$ for R-600a.

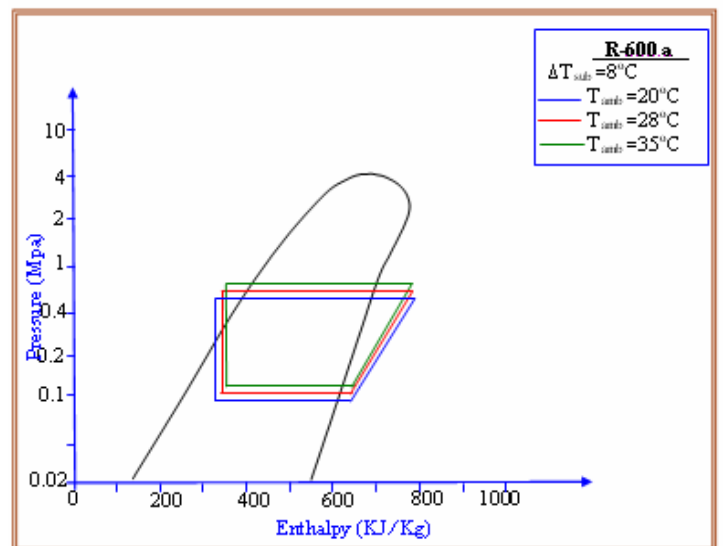


Figure (6.14): Effect of different ambient temperatures on (p-h) diagram at $\Delta T_{sub} = 8^\circ\text{C}$ for R-600a.

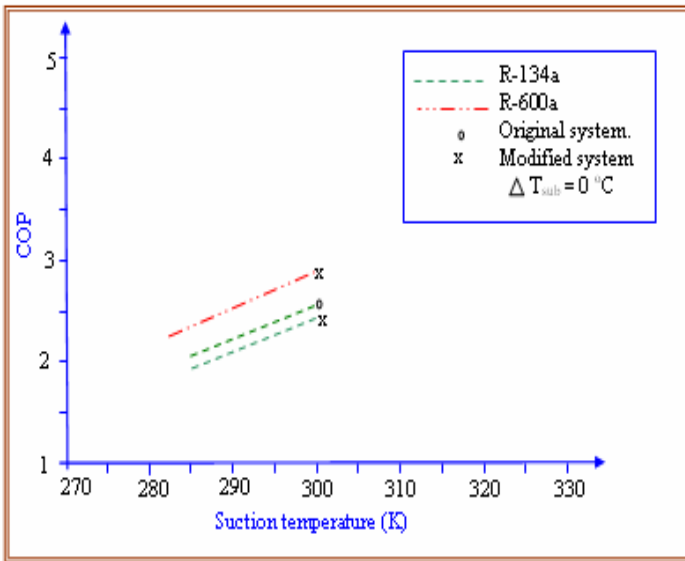


Figure (15): Effect of suction temperature on the COP.

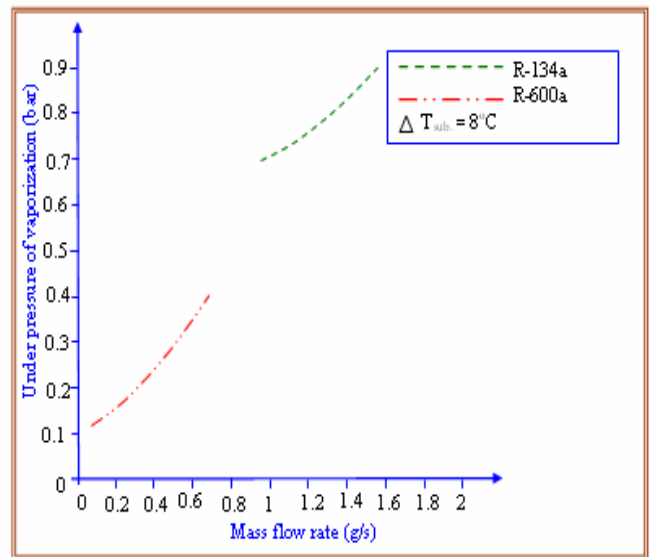


Figure (16): Relationship between underpressure of vaporization and mass flow rate, $\Delta T_{sub} = 8^{\circ}C$.

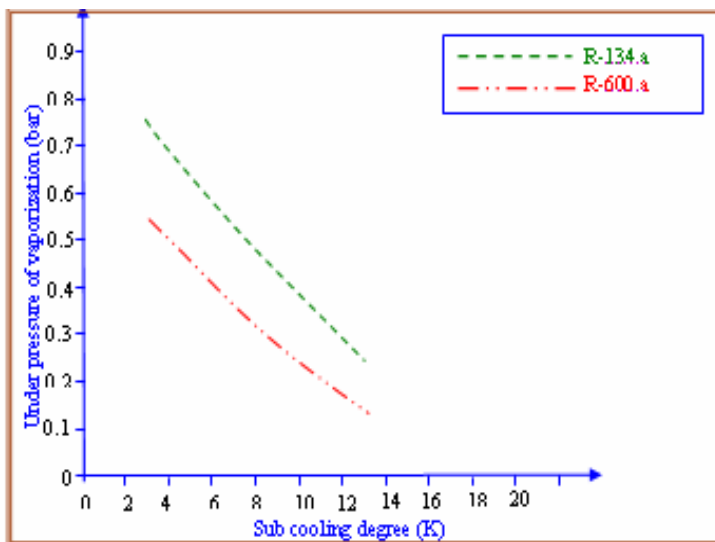


Figure (17): Relationship between underpressure of vaporization and subcooling.

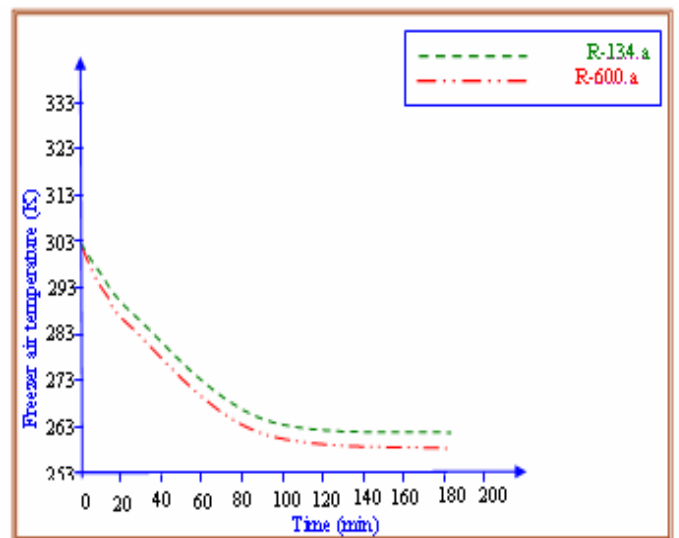


Figure (18): Change freezer air temperature with pull down time for R-134a and R-600a.

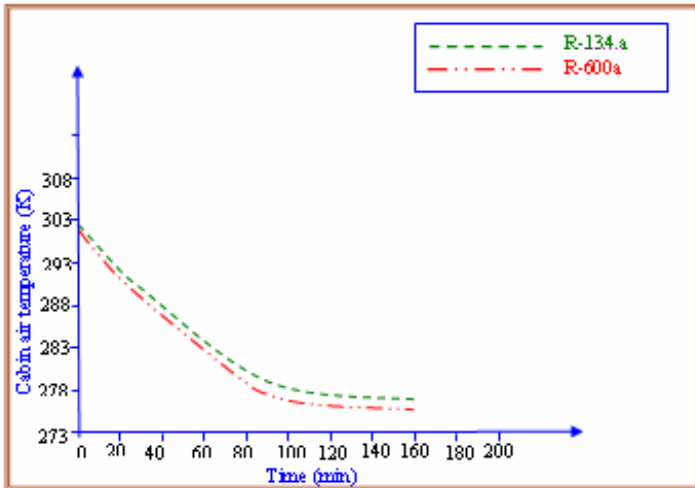


Figure (19): Change cabin air temperature with pull down time for R-134a and R-600a.

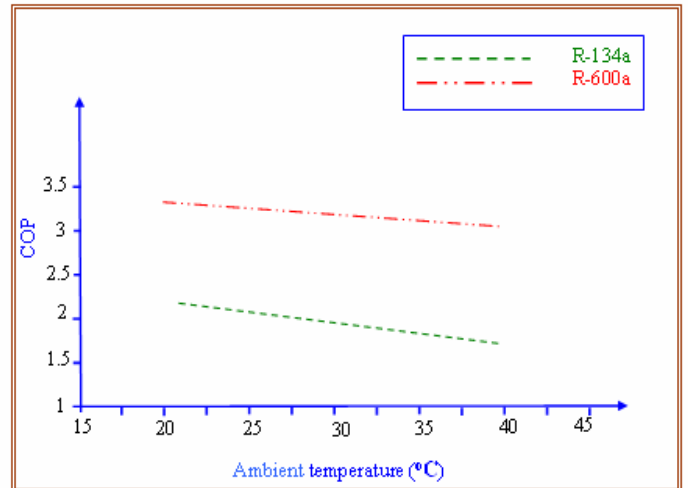


Figure (20): Effect of ambient temperature

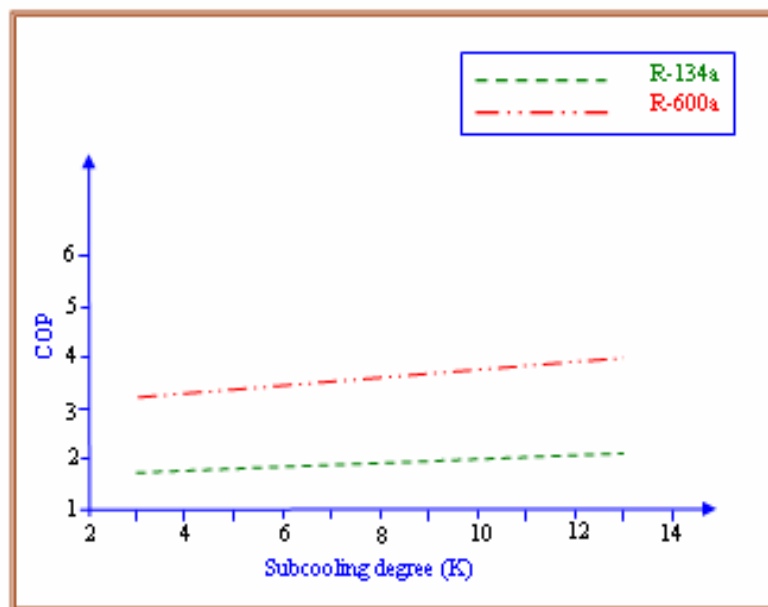


Figure (21): Effect of subcooling degree on the COP.